RAPID COMMUNICATIONS

PHYSICAL REVIEW B VOLUME 46, NUMBER 1 1 JULY 1992-I

Direct correlation between the structure and magnetism of thin epitaxial Fe on Cu(100)

Pascal Xhonneux* and Eric Courtens
IBM Research Division, Zurich Research Laboratory, 8803 Rüschlikon, Switzerland
(Received 26 March 1992)

A systematic study of the structure and magnetism of epitaxial iron films deposited on Cu(100) is reported. For clean room-temperature growth conditions a succession of four different crystalline reconstructions is observed, which appear to be related uniquely to four different magnetic behaviors, as detected by magnon light scattering and the magneto-optical Kerr effect.

There is considerable current interest in thin epitaxial magnetic layers.[1] In particular, numerous studies have been directed at the Fe/Cu(100) system, which in principle allows fcc-Fe films to be produced.[2] The stable phase of Fe at room temperature is bcc, but the extrapolated lattice parameter of fcc-Fe is $\simeq 3.59$ Å, close to that of Cu(100) (3.61 Å). The magnetism of such films has been investigated by spin-polarized photoemission,[3,4] the surface magneto-optic Kerr effect (SMOKE),[5,6] Mössbauer spectroscopy,[7] magnon light scattering (MLS),[8] and scanning electron microscopy with polarization analysis,[9] among others. The structure of such films has been analyzed independently with various elastic[10–12] and inelastic[13,14] techniques, and more recently with scanning tunneling microscopy (STM).[15] In fact, many superstructures have been found that appear to depend *both* on film thickness and on growth conditions, such as substrate temperature and contamination. This may account for the wide variety of results—some apparently contradictory —that are found if the magnetism is correlated solely to the film thickness. This is further complicated by the various growth modes. In the experiments presented in this paper, we use Auger and low-energy electron diffraction (LEED) for growth characterization together with MLS and SMOKE for the determination of the film magnetization. By varying the growth conditions we conclude that a direct correlation exists between the *crystalline reconstructions* of the films and their magnetism.

The films are prepared and characterized in a three-chamber ultrahigh-vacuum (UHV) system allowing *in situ* growth, transfer, and analysis of the magnetic films. The base pressure in the growth chamber is 7×10^{-11} Torr and never exceeds 1.5×10^{-10} Torr during evaporation. The Cu single-crystal substrate is oriented within 1° of the [100] direction as checked by Laue diffraction. After optical quality mechanical polish, it is cleaned in UHV by cycles of gentle Ar^+ sputtering (500 eV) and annealing at 450 °C. After this, the C and O Auger signals are below the detection limit and the LEED shows a sharp (1×1) pattern. The Fe source is constructed like a molecular-beam-epitaxy source except for additional electron-bombardment heating of the iron which is directly sublimated from a high-purity rod. The temperature stability is within ± 1 °C at 1050 °C. The deposition rate is 0.3 atomic layers (AL) per minute as calibrated by three independent methods: Auger, scanning profilometry, and optical transmission of thick films deposited on glass. The C and O contamination in the layer is below 1%, which is just above the detection limit. In a first series of experiments, the substrate temperature is kept at 300 K during growth. Chambliss, Wilson, and Chiang recently observed that under these conditions, layer-by-layer growth takes place up to at least 4 AL with some intermixing of Fe and Cu during growth within the first layer only.[15] We also systematically checked that appreciable interdiffusion of Fe and Cu does not occur at 300 K for periods of up to 2 days, as the relative intensities of the Fe (650 eV) and Cu (850 eV) Auger signals remained constant (to better than 0.5%) before and after the MLS measurements.

Figure 1 shows the evolution of the LEED patterns in function of the Fe film thickness. Below 2.5 AL the growth appears to be epitaxial fcc. Above 2.5 AL a reconstruction with an $n\times1$ pattern, where $n\simeq4,\ldots,5$, is observed. Above 6 AL, the reconstruction becomes 2×1, with very elongated new symmetry reflections of very low

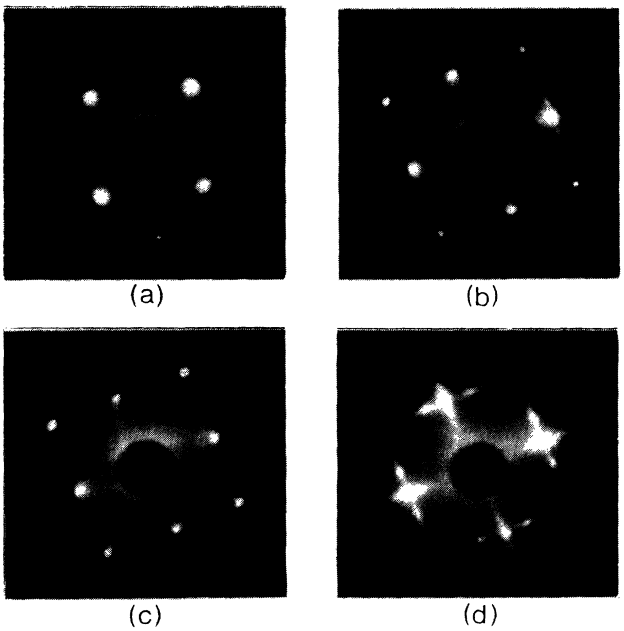

FIG. 1. LEED patterns obtained for epitaxial films of Fe on Cu(100). (a) 2.0 AL (at 123 eV); (b) 3.6 AL (at 113 eV); (c) 9.5 AL (at 115 eV); (d) 20 AL (at 123 eV).

contrast compared to the fcc spots [see Fig. 1(c)]. These reconstructions and the corresponding thicknesses agree with the observations of Landstron *et al.*[11] who reported a 5×1 pattern up to 6 AL, followed by a 2×1 pattern. A 4×1 pattern has also been reported,[16] which we observe only for growth on cooled substrates as described below. These reconstructions, and other similar ones, have recently received much attention.[11–13,17] The patterns can be accounted for by a lateral displacement of top layer atoms.[13] Obviously, the periodicity is frequently interrupted which leads to an appreciable elongation of the spots as seen in Figs. 1(b) and 1(c). The 2×1 pattern is observed up to 17 AL where it suddenly changes markedly as seen in Fig. 1(d). We call the latter reconstruction "pseudo-bcc," because the outside LEED spot positions correspond to the bcc lattice spacing, while remaining spots suggest a coexisting 3×1 structure. Up to 40 AL, both types of spot coexist.

The above results are strongly dependent on growth conditions. For example, a combined oxygen and carbon contamination of about 2% each leads to an immediate 2×2 reconstruction.[14] Under clean growth conditions, and if the substrate surface is not annealed after sputtering (rough surface), the 5×1 reconstruction is not as sharp as in Fig. 1(b), but it persists up to at least 8 AL. Finally, for clean growth on flat substrates cooled to ~120 K, the 5×1 reconstruction gives way to a 4×1 pattern at ~6 AL, and this $n\times1$ structure ($n=4,\ldots,5$) persists up to at least 10 AL. In that case the LEED pattern loses contrast with increasing thickness.

After deposition, samples are transferred in UHV to an analysis chamber whose base pressure is below 5×10^{-11} Torr. Here, MLS and SMOKE are performed. For this purpose, we use a 5145-Å argon laser, and apply a magnetic field H perpendicular to the plane of incidence of the light. The reflected beam is used to perform transverse SMOKE. For MLS the incoming light is polarized in the plane of incidence. The backscattered light is analyzed for its depolarized component and focused on the entrance pinhole of a tandem six-pass Fabry-Pérot interferometer of very high contrast and luminosity.[18] Typical spectra are illustrated in Fig. 2. The peak centered at zero frequency is due primarily to elastically scattered light which is used to maintain the tuning of the instrument. It is much larger than the inelastic signal, and is not shown in Fig. 2. The peaks at frequency shifts $\pm\omega$ to the left and right of the central peak correspond to creation and annihilation of a magnon, respectively. No phonon contributions are seen owing to the polarization selection rules. MLS is an excellent technique to observe magnetic excitations,[19] as it is sensitive down to the monolayer.[20]

We performed MLS on numerous films corresponding to the structures of Fig. 1. Films below 2.5 AL show neither magnon peaks nor transverse SMOKE signals, which also hold true upon cooling down to 160 K. Well reconstructed 5×1 films (between 3 and 6 AL) show an MLS signal of the type illustrated in Fig. 2(a). At low field the magnon peaks are broad and $\omega(H)$ decreases with increasing field, as shown in Fig. 3(a). Beyond a critical field H_{cr} the magnon peaks become narrow and their frequency dependence is reversed. This indicates that the zero-field magnetization is out of plane and that it tilts in plane at H_{cr}.[8] Above 6 AL, the 2×1 reconstructed films do not show magnon peaks within the range ~1 to ~1000 GHz, and from room temperature down to ~160 K. Neither are we able to detect a transverse SMOKE signal. Polar SMOKE signals and spin-polarized photoemission have been reported for this thickness range, with an anomalous decrease of the Curie temperature with increasing thickness.[5,21] Above 17 AL, the pseudo-bcc reconstruction leads to the signals shown in Figs. 2(b) and 3(b). The monotonic dependence of ω on H indicates an in-plane magnetization.

The data from Fig. 3(a) are fitted using the magnetostatic approximation and taking into account the first- (K_{u1}) and second- (K_{u2}) order uniaxial anisotropies.[8] The exchange in the layer is negligible owing to the small scattering wave vector ($q=1.73\times10^5$ cm^{-1}).[22,23] The second-order uniaxial anisotropy affects the $\omega(H)$ dependence only in the out-of-plane regime [the dashed line in Fig. 3 is for $K_{u2}=0$]. In order to obtain good fits we had to allow the gyromagnetic ratio g to be a free parameter. The fits gave values for g always lower than 2.1, sometimes as low as 1.4, an unexpected result for iron.[24,25]

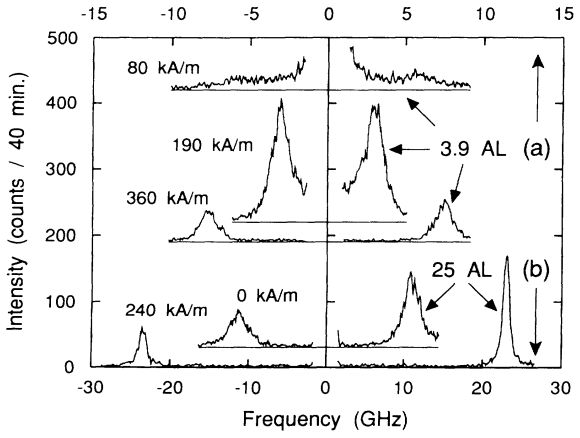

FIG. 2. MLS spectra obtained on two different film thicknesses and at several fields, as indicated in (a) and (b). The in-plane scattering vector is $q=1.73\times10^5$ cm^{-1}.

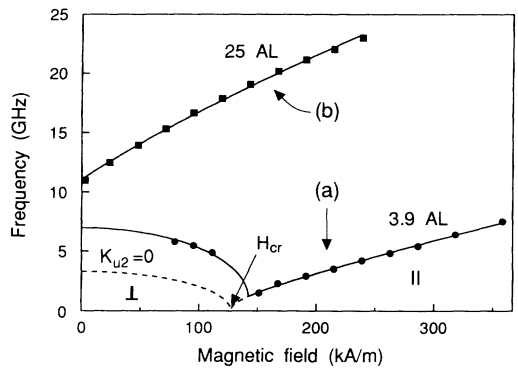

FIG. 3. The dependence of the magnon frequency on the applied field for the two films, shown by (a) and (b), in Fig. 2. The fits are explained in the text.

Such low g factors were already reported for similar layers covered with copper.[26] The most likely origin for this difficulty lies, we believe, in the spatial variation of the uniaxial anisotropy. The first uniaxial anisotropy constant is proportional to a surface anisotropy K_s and inversely proportional to the film thickness s, $K_{u1}=K_s/s$. Spatial inhomogeneity of these films, even for an integer number of layers, is expected due to growth in patches.[15] A variation of ± 1 AL on a 3 AL film produces then a strong fluctuation on K_{u1}, which reduces the significance of fitting with a homogeneous-thin-slab model. However, the field H_{cr} at which $\omega(H)$ reaches its minimum [see Fig. 3(a)] does not depend on g. The corresponding effective saturation magnetization, $-H_{cr}=(M_s)_{eff}\equiv M_s-2\bar{K}_{u1}/\mu_0 M_s$, defines a mean value of the uniaxial anisotropy constant $\bar{K}_{u1}$. The effective magnetization has been plotted in Fig. 4. The frequencies from pseudo-bcc films are well fitted with $g=2.1$ [solid line in Fig. 3(b)], when we allow only for first-order magnetocrystalline anisotropy K_1 in the magnetostatic approximation. We have measured that the easy magnetization axis lies along the [100] direction of the copper substrate. For the measurements shown here the magnetic field was applied in that direction. The only fit parameters were the saturation magnetization M_s and K_1. The resulting magnetizations are shown in Fig. 4. The corresponding values of K_1 increase with thickness, from 0.36 to 0.54×10^5 J/m^3, remaining close to the iron bulk value of 0.42×10^5 (Ref. 27). The measured coercitive fields for these layers are above 5 kA/m.

Each symbol in Fig. 4 is measured for a different film. Films for which no MLS signal was obtained are shown by symbols on the abscissa. We know that our spectrometer is sufficiently sensitive to detect a ferromagnetic signal in very thin films. For example, a 2×2 reconstructed Fe film of ~2 AL exhibited a strong magnon peak with an $\omega(H)$ dependence typical for in-plane ferromagnetism. The absence of a MLS signal is thus a strong indication for the absence of usual ferromagnetism. For the thinner films in Fig. 4, this is in qualitative agreement with the results of Liu, Moog, and Bader[5] and suggests that the Curie temperature is indeed very low.[21] For the films that exhibit a 5×1 reconstruction, after a rapid onset the absolute value of the effective magnetization shows a clear tendency to decrease for the thicker films. Forcing the $n\times1$ structure ($n=4$ or 5) to persist to thicknesses above 6 AL by evaporation on either a cold or rough substrate as explained above, this behavior of the effective magnetization was found to continue, thus yielding in-plane signals from $\simeq6$ AL on. By contrast, as soon as the 2×1 reconstruction is observed, no MLS signal is obtained. The latter films are clearly not ferromagnetic in the usual sense, although films in this thickness range have been reported to give polar Kerr signals as well as spin-polarized photoemission.[5,21] In fact, we find that in the range from ~6 to at least 10 AL, films can be prepared with two different crystalline reconstructions which exhibit correspondingly

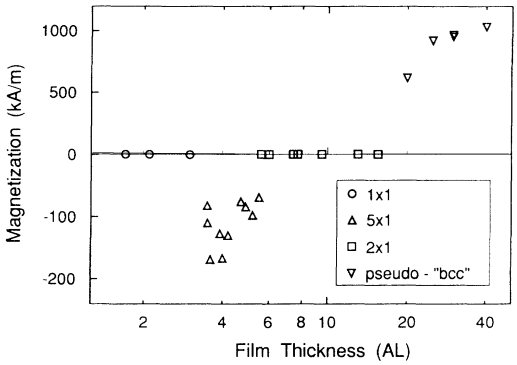

FIG. 4. The effective magnetization at zero field derived from MLS spectra as a function of film thickness. The different symbols correspond to different structures as observed in LEED. The negative magnetization scale is expanded by a factor of 5.

distinct magnetic properties. Our observation of a change of magnetic regime around 6 AL is consistent with the structural result of Magnan *et al.*[12] who reported that even the first iron layers at the interface with the copper must reorder when the thickness of the iron is increased from 3.5 to 8.4 AL. The films above 17 AL have a magnetization which increases with thickness, but remains about 0.6 times the bulk value. This is presumably related to the structural difference between these films and bulk bcc.

This evolution of magnetization with film thickness is rather surprising, and it appears to be clearly related to relatively minor changes in the LEED patterns. The above observations establish a direct correlation between magnetism and details of the crystalline structure for Fe films on Cu(100). Spin-polarized band-structure calculations of bulk fcc Fe have indicated the possibility that several different magnetic states exist depending on small changes of the lattice parameter: nonmagnetic, low-spin ferromagnet, antiferromagnet, and high-spin ferromagnet.[28] Clearly the reconstructed films have a more complicated structure than bulk fcc, but different reconstructions could clearly correspond to different effective lattice parameters. Our results emphasize the importance of observing the structure in magnetic studies of thin epitaxial films. Much remains to be done to understand these observations in detail, particularly in relation to the evasive magnetism of the 2×1 reconstructed films. Also, a careful STM measurement of the topography could presumably establish the real-space atomic ordering related to the LEED patterns.

The authors thank H. C. Siegmann and R. Allenspach for numerous discussions and a careful reading of the manuscript, S. Alvarado and E. Tosatti for helpful conversations, and B. Weiss for technical assistance with the design and realization of the UHV system.

*Also at the Laboratorium für Festkörperphysik, Eidgenössische Technische Hochschule, Zürich-Hönggerberg, Switzerland.

[1]See, e.g., *Magnetism in Ultrathin Films,* edited by D. Pescia [Appl. Phys. A **49**, (1989), special issue].

[2]W. A. Jesser and J. W. Matthews, Philos. Mag. **15**, 1097 (1967).

[3]D. Pescia, M. Stampanoni, G. L. Bona, A. Vaterlaus, R. F. Willis, and F. Meier, Phys. Rev. Lett. **58**, 2126 (1987).

[4]D. P. Pappas, K.-P. Kämper, and H. Hopster, Phys. Rev. Lett. **64**, 3179 (1990).

[5]C. Liu, E. R. Moog, and S. D. Bader, Phys. Rev. Lett. **60**, 2422 (1988).

[6]W. R. Bennett, W. Schwarzacher, and W. F. Egelhoff, Jr., Phys. Rev. Lett. **65**, 3169 (1990).

[7]W. A. A. Macedo and W. Keune, Phys. Rev. Lett. **61**, 475 (1988), and references therein.

[8]J. R. Dutcher, B. Heinrich, J. F. Cochran, D. A. Steigerwald, and W. F. Egelhoff, Jr., J. Appl. Phys. **63**, 3464 (1988).

[9]M. Stampanoni and R. Allenspach, J. Magn. Magn. Mater. **104-107**, 1805 (1992).

[10]S. H. Lu, J. Quinn, D. Tian, F. Jona, and P. M. Marcus, Surf. Sci. **209**, 364 (1989), and references therein.

[11]H. Landstron, G. Schmidt, K. Heinz, K. Müller, C. Stuhlmann, U. Beckers, M. Wuttig, and H. Ibach, Surf. Sci. **256**, 115 (1991).

[12]H. Magnan, D. Chandesris, B. Vilette, O. Heckmann, and J. Lecante, Phys. Rev. Lett. **67**, 859 (1991).

[13]W. Daum, C. Stuhlmann, and H. Ibach, Phys. Rev. Lett. **60**, 2741 (1988).

[14]D. A. Steigerwald, I. Jacob, and W. F. Egelhoff, Jr., Surf. Sci. **202**, 472 (1988).

[15]D. D. Chambliss, R. J. Wilson, and S. Chiang, J. Vac. Sci. Technol. A (to be published).

[16]C. Egawa, E. McCash, and R. F. Willis, Surf. Sci. **215**, L271 (1989).

[17]F. Ercolessi, E. Tosatti, and M. Parrinello, Phys. Rev. Lett. **57**, 719 (1986).

[18]J. Sandercock, in *Light Scattering in Solids III,* edited by M. Cardona and G. Güntherodt, Topics in Applied Physics Vol. 51 (Springer, Berlin, 1982), p. 173.

[19]P. Grünberg, Prog. Surf. Sci. **18**, 1 (1985).

[20]D. Kerkmann, J. A. Wolf, D. Pescia, Th. Woike, and P. Grünberg, Solid State Commun. **72**, 963 (1989).

[21]M. Stampanoni, Appl. Phys. A **49**, 449 (1989).

[22]R. L. Stamps and B. Hillebrands, Phys. Rev. B **44**, 5095 (1991).

[23]J. F. Cochran, W. B. Muir, J. M. Rudd, B. Heinrich, Z. Celinski, Tan-Trung Le-Tran, W. Schwarzacher, W. Bennett, and W. F. Egelhoff, Jr., J. Appl. Phys. **69**, 5206 (1991).

[24]C. Kittel, Phys. Rev. B **76**, 743 (1949).

[25]J. H. Van Vleck, Phys. Rev. B **78**, 266 (1950).

[26]J. R. Dutcher, Ph.D. thesis, Simon Fraser University, 1988.

[27]C. Kittel, *Introduction to Solid State Physics* (Wiley, New York, 1976).

[28]V. L. Moruzzi and P. M. Marcus, in *Handbook of Ferromagnetic Materials,* 2nd ed., edited by K. Buschow (Elsevier, Amsterdam, 1992).

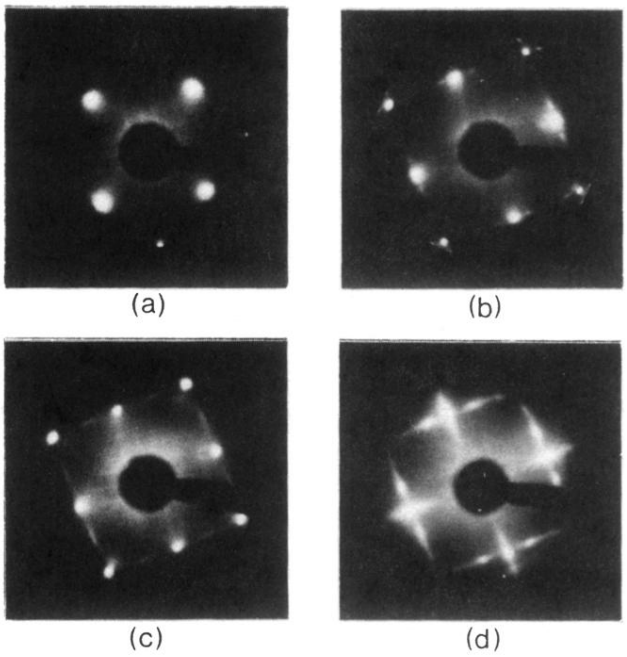

FIG. 1. LEED patterns obtained for epitaxial films of Fe on Cu(100). (a) 2.0 AL (at 123 eV); (b) 3.6 AL (at 113 eV); (c) 9.5 AL (at 115 eV); (d) 20 AL (at 123 eV).